Chemico-Biological Interactions 222 (2014) 87–96

Contents lists available at ScienceDirect

Chemico-Biological Interactions

journal homepage: www.elsevier.com/locate/chembioint

Polyoxometalates as antitumor agents: Bioactivity of a new polyoxometalate with copper on a human osteosarcoma model

I.E. León [a], V. Porro [b], S. Astrada [b], M.G. Egusquiza [c], C.I. Cabello [c], M. Bollati-Fogolin [b], S.B. Etcheverry [a,*]

[a] Centro de Química Inorgánica (CONICET-UNLP), Facultad de Ciencias Exactas, Universidad Nacional de La Plata, 47 y 115, 1900 La Plata, Argentina
[b] Unidad de Biología Celular, Institut Pasteur de Montevideo, Mataojo 2020, Montevideo, 11400, Uruguay
[c] Centro de Investigación y Desarrollo en Ciencias Aplicadas CINDECA, La Plata, Argentina

ARTICLE INFO

Article history:
Received 11 January 2014
Received in revised form 8 October 2014
Accepted 10 October 2014
Available online 22 October 2014

Keywords:
Anticancer drug
MG-63 human osteosarcoma cells
Mechanisms of action
Polyoxometalates
Copper

ABSTRACT

Polyoxometalates (POMs) are early transition metal oxygen anion clusters. They display interesting biological effects mainly related to their antiviral and antitumor properties. On the other hand, copper compounds also show different biological and pharmacological effects in cell culture and in animal models. We report herein for the first time, a detailed study of the mechanisms of action of a copper(II) compound of the group of HPOMs with the formula $K_7Na_3[Cu_4(H_2O)_2(PW_9O_{34})_2]20H_2O$ (PW_9Cu), in a model of human osteosarcoma derived cell line, MG-63. The compound inhibited selectively the viability of the osteosarcoma cells in the range of 25–100 μM ($p < 0.01$). Besides, we have clearly shown a more deleterious action of PW_9Cu on tumor osteoblasts than in normal cells. Cytotoxicity studies also showed deleterious effects for PW_9Cu. The increment of reactive oxygen species (ROS) and the decrease of the GSH/GSSG ratio were involved in the antiproliferative effects of PW_9Cu. Moreover, the compound caused cell cycle arrest in G_2 phase, triggering apoptosis as determined by flow cytometry. As a whole, these results showed the main mechanisms of the deleterious effects of PW_9Cu in the osteosarcoma cell line MG-63, demonstrating that this compound is a promissory agent for cancer treatments.

1. Introduction

Polyoxometalates (POMs) are early transition metal oxygen anion clusters. They are aggregates of metal cations (usually the d^0 species V(V), Nb(V), Ta(V), Mo(VI), and W(VI)) bridged by oxide anions [1].

In addition, the heteropolyoxometalates (HPOMs) contain one or more heteroatoms (e.g.: P, Cu, Si, Ge, As, etc.). The structural, electronic properties as well as their easily modified physicochemical characteristics (polarity, redox potential, surface charge distribution, shape, and stability under physiological conditions), make them attractive for several applications in different fields, specially as pharmaceutical drugs.

From a medical point of view, the HPOMs are very interesting compounds due to their antiviral and antitumor effects [2,3]. The first biological report on the antiviral activity of POMs was published in 1971 [4]. Then, several scientific papers about this subject have been reported with special focus on their activity against Human Inmmunodeficiency Virus (HIV) [5–7].

During the last decades, studies of biomedical activity of inorganic precursors of POMs like molybdenum and vanadium compounds have attracted the attention of numerous investigators [2,8–10]. Moreover, reviews about bioactivity of tungsten compounds are infrequent [11–13].

The biomedical importance of the POMs, is mainly based on their interaction with enzymes such as alkaline phosphatase [14], growth factors [15] and cellular constituents [16].

The pharmacological applications of HPOMs as inorganic pharmaceuticals are still rare compared to the far more common organic compounds [17]. Due to the lack of a thorough understanding of the biological mechanisms used by POMs, the investigation of their mechanisms of action constitutes an attractive field for research.

In the present work, we have chosen the MG-63 cell line derived from a human osteosarcoma because, according to the literature, it is a good model and one of the most used lines for bone cancer research [18,19].

On the other hand, copper is an essential transition element that plays a crucial role in the biochemistry of all aerobic organisms [20]. Moreover, copper plays a role as an anti-inflammatory agent and also, many complexing agents, which are pharmacologically inactive by themselves, display anti-inflammatory properties

* Corresponding author.
E-mail address: etcheverry@biol.unlp.edu.ar (S.B. Etcheverry).

http://dx.doi.org/10.1016/j.cbi.2014.10.012
0009-2797/

in association with copper(II) [20–23]. Cancer has been described as a disease associated with an inflammatory response [24]. Indeed, numerous copper complexes that demonstrated Superoxide Dismutase (SOD)-mimetic properties have shown anticancer, anticarcinogenic, and antimutagenic effects both *in vitro* and *in vivo* [25]. For these reasons, it is worthy to understand the mechanisms of action of copper compounds in relation to cancer treatment.

According to literature, the present study deals, for the first time, with the effects of a copper(II) heteropolytungstate as a potential antitumor compound in osteoblast like cells. The selected heteropolytungstate $K_7Na_3[Cu_4(H_2O)_2(PW_9O_{34})_2]20H_2O$ (in advance PW_9Cu) belongs to an isomorphic series $[(PW_9O_{34})_2M_4]^{10-}$ with M = Cu(II).

The effects of this compound on the viability of the tumor cell line MG-63, are herein reported. We have investigated the putative mechanisms involved in its antiproliferative effects, with particular focus on the role of oxidative stress (ROS induction) and on the disturbance of GSH/GSSG ratio. Cytotoxicity, mainly at lysosomes and mitochondria metabolism, has been also studied. Finally, cell cycle distribution and apoptosis induction have been investigating using flow cytometry and confocal microscopy.

2. Materials and methods

2.1. Materials

Tissue culture materials were purchased from Corning (Princeton, NJ, USA), Dulbecco's Modified Eagles Medium (DMEM), TrypLE™ from Gibco (Gaithersburg, MD, USA), and fetal bovine serum (FBS) from Internegocios SA (Argentina). Dihydrorhodamine 123 (DHR) was purchased from Molecular Probes (Eugene, OR). Annexin V, Fluorescein isothiocyanate (FITC), rhodamine 123, propidium iodide (PI), CellMask™ and TOPRO-3 were from Invitrogen Corporation (Buenos Aires, Argentina). Reduced glutathione (GSH) and Vitamin E (α-Tocopherol) were purchased from Sigma Chemical Co. (St. Louis, MO, USA). Ascorbic acid (Vitamin C) was purchased from Merck Argentina (Buenos Aires, Argentina).

All other chemical were from Sigma Chemical Co. (ST. Louis, MO).

MC3T3-E1, UMR106, MG-63 cell lines were purchased from *ATCC*.

2.2. Synthesis of $K_7Na_3[Cu_4(H_2O)_2(PW_90_{34})_2]20H_2O$

$K_7Na_3[Cu_4(H_2O)_2(PW_90_{34})_2]20H_2O$ was synthesized according to Finke et al. [26]. Briefly, 5 g (1.8 mmol) of the precursor Na8H[PW9O34]19H2O (PW9) thermally treated (60 °C for three days in air atmosphere) were added to 12 mL of an aqueous solution of CuCl2·2H2O (6.2 g or 3.6 mmol) followed by the addition of an excess of solid KCl (0.66 g, 8.8 mmol). The slightly cloudy solution was centrifuged for about 5 min. The clear light green supernatant was removed and allowed to crystallize at room temperature. The crystals were recrystallized in water, air-dried and characterized. The product obtained was characterized as previously reported [27,28].

2.3. Preparation of $K_7Na_3[Cu_4(H_2O)_2(PW_90_{34})_2]20H_2O$ solutions

Fresh stock solutions of the complex were prepared in distilled water at 10 mM and diluted according to the concentrations indicated in the legends of the figures.

2.4. Stability of the PW_9Cu in solution

To test the stability of PW_9Cu we analyzed the UV–visible spectra at 2.5 mM. The electronic spectra were recorded at times ranging from 0 to 48 h. The stability of the complex was followed at 816 nm by spectrophotometric measurement using a UV–vis Hewlett–Packard, Palo Alto, CA, USA, 8453 spectrophotometer.

2.5. Cell lines and growth conditions

MC3T3-E1, UMR106, and MG-63 osteoblast like cells were grown in DMEM containing 10% FBS, 100 U/mL penicillin and 100 μg/mL streptomycin at 37 °C in 5% CO_2 atmosphere. Cells were seeded in a 75 cm^2 flask and when 70–80% of confluence was reached, the cells were subcultured using 1 mL of TrypLE™ per each 25 cm^2 flask. For experiments, the cells were grown in different multi-well plates according to the assays: 48 wells for cell viability test, 96 for MTT and NR assays, 24 for ROS and GSH measurements, 12 for apoptosis determinations and 6 for cell cycle analysis. When the cells reached the desired confluence, the monolayers were washed with DMEM and were incubated under different conditions according to the experiments.

2.6. Cell viability: crystal violet assay

A mitogenic bioassay was carried out as described by Okajima et al. [29] with some modifications. Briefly, cells were grown in 48 well plates. For experiments, 3×10^4 cells/mL were grown for 24 h at 37 °C in 5% CO_2 atmosphere. Then, the monolayers were incubated for 24 h with different concentrations (2.5–100 μM) of the free ligand or the compound PW_9Cu. Besides, incubations were also carried out with PW_9Cu plus reduced glutathione (GSH) or with a mixture of vitamins C and E. Cells were preincubated with GSH (1 mM) during 2 h. Then, the thiol was eliminated before the addition of PW_9Cu. For other experiments the cells were incubated with different concentrations of the compound plus a mixture of vitamins C and E (50 μM each) during 24 h.

After this treatment, the monolayers were washed with PBS and fixed with 5% glutaraldehyde/PBS at room temperature for 10 min. After that, the cells were stained with 0.5% crystal violet/25% methanol for 10 min. Then, the dye solution was discarded and the cells were washed with water and dried. The dye taken up by the cells was extracted using 0.5 mL/well 0.1 M glycine/HCl buffer, pH 3.0/30% methanol and transferred to test tubes. After a convenient sample dilution the absorbance was read at 540 nm. It had been previously reported that under these conditions, the colorimetric bioassay strongly correlated with cell proliferation measured by cell counting in Neubauer chamber [30].

2.7. MTT assay

The MTT assay was performed according to Mosmann [31]. Briefly, cells were seeded in a 96-multiwell dish (2.5×10^4 cells per well), allowed to attach for 24 h and treated with different concentrations of PW_9Cu at 37 °C for 24 h. After that, the medium was changed and the cells were incubated with 0.5 mg/mL MTT under normal culture conditions for 3 h. Cell viability was determined by the conversion of the tetrazolium salt MTT (3-(4,5-dimethylthiazol-2-yl)-2,5-diphenyl-tetrazolium-bromide) to a colored formazan by mitochondrial dehydrogenases. Color development was measured spectrophotometrically at 570 nm in a Microplate Reader (7530, Cambridge technology, Inc, USA) after cell lysis in DMSO (100 μL/well). Cell viability was plotted as the percentage of the control value.

2.8. Neutral red assay

The neutral red accumulation assay was performed according to Borenfreund and co-workers [32]. Cells were plated into 96 well culture plates (2.5×10^4 cells per well) and treated with different PW_9Cu concentrations for 24 h at 37 °C in 5% CO_2 in air. After treatment, the medium was replaced by another containing 100 μg mL^{-1} neutral red (NR) dye. After that, the cells were incubated for 3 h at 37 °C. Then, the neutral red medium was discarded, the cells were rinsed twice with warm PBS (37 °C, pH 7.4) to remove the non-incorporated dye. 100 μL of a 50% ethanol and 1% acetic acid solution were added to each well to fix the cells releasing the NR into the solution. The plates were shaken for 10 min and the absorbance of the solution in each well was measured at 540 nm in a microplate reader (7530, Cambridge Technology, Inc., USA). Optical density was plotted as a percentage of the control wells (without any treatment).

2.9. Mechanism of action

2.9.1. Determination of reactive oxygen species (ROS) production

Intracellular ROS generation in osteoblasts was measured by oxidation of dihydrorhodamine 123 (DHR123) to rhodamine by spectrofluorescence. Cells were incubated for 30 min at 37 °C in 1.5 mL of Hank's buffered salt solution alone (basal condition) or with the compound in the presence of 10 mM DHR123 [33]. Media were separated and the cell monolayers rinsed with PBS and lysated by means of 1 mL of 0.1% Triton X-100. The cell extracts were then analyzed to determine the oxidized product (rhodamine) by measuring fluorescence (excitation wavelength 500 nm, emission wavelength 536 nm), using a Perkin–Elmer LS 50B spectrofluorometer. The results were corrected for protein content, which was assessed by the method of Bradford [34].

2.9.2. Fluorometric determination of cellular GSH and GSSG levels

GSH and GSSG levels were determined in osteoblasts in culture as follows. Confluent osteoblast monolayers from 24 well dishes were incubated with different concentrations of PW_9Cu at 37 °C for 24 h. Then, the monolayers were washed with PBS and harvested by incubating them with 250 μL Triton 0.1% for 30 min. For GSH determination, 100 μL aliquots were mixed with 1.8 mL of ice cold phosphate buffer (Na_2HPO_4 0.1 M-EDTA 0.005 M pH 8) and 100 μL o-phthaldialdehyde (0.1% in methanol) as it was described by Hissin and Hilf [35]. For the determination of GSSG, 100 μL aliquots were mixed with 1.8 mL NaOH 0.1 M and o-phthaldialdehyde as before. Previously, to avoid GSH oxidation, the cellular extracts for GSSG determination were incubated with 0.04 M of N-ethylmaleimide (NEM). Fluorescence at an emission wavelength of 420 nm was determined after excitation at 350 nm.

GSH/GSSG ratio, which is a better marker for the cellular redox status than GSH alone, was calculated as % of the basal for all the experimental conditions.

2.9.3. Measurement of the exposure of phosphatidyl serine (PS) by annexin V-FITC/PI staining

Cells in early and late stages of apoptosis were detected by Annexin V-FITC and Propidium Iodide (PI) staining. Cells were treated with 25 and 100 μM PW_9Cu and incubated for 24 h prior to analysis.

For staining, cells were washed with PBS and adjusted to a concentration of 1×10^6 cell/mL in 1 × binding buffer (0.01 M HEPES, pH 7.4; 0.14 M NaCl; 2.5 mM $CaCl_2$). To 100 μL of cell suspension, 2.5 μL of Annexin V-FITC were added and incubated for 15 min at room temperature. Finally, 2 μL PI (250 μg/mL) were added prior to analysis. Cells were analyzed using a flow cytometer CyAnTM ADP (Beckman Coulter, USA) and Summit v4.3 software. For each analysis 10,000 counts, gated on a FSC vs SSC dot plot, were recorded. In the Annexin V-FITC vs PI dot plot, gate strategy was applied to identify cell subpopulations: the undamaged vital (Annexin V−/PI−), the vital mechanically damaged (Annexin V−/PI+), the apoptotic (Annexin V+/PI−), and the secondary necrotic (Annexin V+/PI+).

2.9.4. Measurement of cell cycle/DNA content

DNA content in G_1/G_0, S, G_2/M phases was analyzed using flow cytometry [36,37].

Cells were seeded on 6 well plates, cultured during 24 h and then treated with 25 μM and 100 μM of PW_9Cu for 6 and 24 h. The harvested cells were washed with PBS, fixed and permeabilized with 70% ice-cold ethanol for more than 2 h. Subsequently, the cells were resuspended in a freshly staining buffer (final concentration of 50 μg/mL of PI and 50 μg /mL DNase-free RNase prepared in PBS containing 2 mM EDTA) and incubated for 30 min at 37 °C. Cell cycle distribution analysis was performed in a CyAnTM ADP flow cytometer using Summit v4.3 software for data acquisition. For each sample, cellular aggregates were gating out and at least 10,000 cells were counted and plotted on a single parameter histogram. The percentage of cells in the G_1/Go, S, G_2/M phases and sub-G_1 peak was then calculated by FlowJo 7.6 software (using the Watson model).

2.9.5. Cell morphology

MG-63 cells were seeded in 6 well-plates containing cover slips (2×10^5 cell/well) and were culture in DMEM-Glutamax, 10% fetal bovine serum, at 37 °C for 24 h. Subsequently, PW_9Cu was added to a final concentration of 25 and 100 μM. Cells were incubated for 6 and 24 h at 37 °C, then the cover slips were washed with PBS, the cells were fixed in 4% paraformaldehyde for 15 min and washed with a Tween 20 solution (0.2% in PBS). CellMask™ (1:2000, Invitrogen) and TOPRO-3 (1:1000, Invitrogen) were used to count stained cell membranes and nuclei, respectively. All images were taken using laser confocal microscope Leica TCS SP5 and a 63× oil objective. Five optical sections scanned at intervals of 0.3 μm were taken per sample projected using the Maximum Intensity Model and colored with predetermined Lut (red or blue) provided by the LASAF Lite 2.6.0v software.

2.9.6. Mitochondrial membrane potential (MMP)

Mitochondrial membrane potential was determined by the uptake of Rhodamine 123 according to the method of Wu and col [38].

The cells cultured on 96-well plates, were washed in PBS and incubated with 5 μg/ml Rhodamine 123 for 30 min at 37 °C. After further washing, the cells were incubated with DMEM for 30 min. Ethanol/Water 1/1 solution was used to extract the amount of dye retained by the cells. For the control tube, add 1 μL of 50 mM carbonyl cyanide m-chlorophenylhydrazone (CCCP, 50 μM final concentration) and incubate the cells at 37 °C for 5 min. The changes in MMP were analyzed by fluorescence spectroscopy (Spectra max M from Molecular Devices), with an excitation wavelength of 485 nm and an emission wavelength of 530 nm

2.10. Statistical analysis

At least three independent experiments were performed for each experimental condition in all the biological assays. The results are expressed as the mean ± the standard error of the mean (SEM). Statistical differences were analyzed using the analysis of variance method (ANOVA) followed by the test of least significant difference (Fisher).

3. Results

3.1. Synthesis and stability study

PW_9Cu (Fig. 1) was synthesized according to Finke et al. [26]. The obtained powder sample of the compound was identified by Fourier Transformed Infrared spectroscopy (FTIR). The solid sample was stable at least six months as determined by FTIR.

For biological tests, PW_9Cu was dissolved in distilled water and the stability of the solutions was assessed by means of pH measurements and UV–vis spectroscopy. The results showed that the solutions were stable for 24 and 48 h, (times used in the biological experiments). The UV–vis spectra showed that the most intense band, centered at about 261 nm, can be undoubtedly assigned to a O → W charge transfer transition [39]. The weaker band, located at 816 nm, is evidently related to "d–d" transitions of the Cu(II) cation. This relatively broad band is assigned to the $2E_g \rightarrow 2T_{2g}$ transition, characteristic for Cu(II) in an octahedral environment [40].

3.2. Effect of HPOMS on cell viability

To study the effect of PW9Cu on osteoblast like cell viability, three different cell lines were selected: a normal osteoblast cell line derived from mouse calvaria (MC3T3-E1) used as a control culture and two tumor cell lines, one derived from a rat osteosarcoma (UMR106) an the other from a human osteosarcoma (MG-63).

PW_9Cu has impaired the cell viability from 20 μM in MG-63 cells ($p < 0.01$) as shown in Fig. 2A. On the other hand, UMR106 osteosarcoma murine cell line showed a decrease viability in the range of 50–100 μM ($p < 0.01$). On the contrary, the antiproliferative actions of the compound in normal osteoblastic cells (MC3T3-E1) did not show any significant differences from 25 to 75 μM concentration range while at 100 μM a significant deleterious action was detected ($p < 0.01$). The damaging effect of PW_9Cu on the three osteoblastic cell lines showed the following increasing potency: MC3T3-E1 < UMR106 < MG-63, with IC_{50} values of: 92, 81 and 22 μM, respectively.

As a whole, these results indicate that PW_9Cu caused greater antiproliferative action on tumor cell lines than on normal osteoblasts. Moreover, among the tumor cells, the compound caused the strongest antiproliferative action in the human derived osteosarcoma cells. The strongest effect of PW_9Cu on MG-63 cell line allows us to consider this compound as an interesting candidate for potential antitumor uses.

To estimate the potency of PW_9Cu as antitumor agent, we compare its effects with the anticancer reference drug *cis*-Pt. In Fig. 2B it can be observed that PW_9Cu caused a more pronounced antiproliferative effect than *cis*-Pt on the human osteosarcoma cell line. At 25 μM PW_9Cu provoked a decrease of 60% in cell viability while *cis*-Pt generated only ca. 15% inhibition of cell proliferation ($p < 0.01$).

The comparison of IC_{50} values (22 *vs.* 43 μM) for these two antitumor drugs showed that PW9Cu displayed a greater significant effectiveness as antitumor agent in MG-63 cell line.

Considering the selective antitumor action of PW_9Cu on the studied osteoblast cell lines, the cytotoxicity of this compound as well as the putative mechanisms of action were thoroughly investigated only in MG-63 osteosarcoma cells since in these cells it caused the strongest antitumor action.

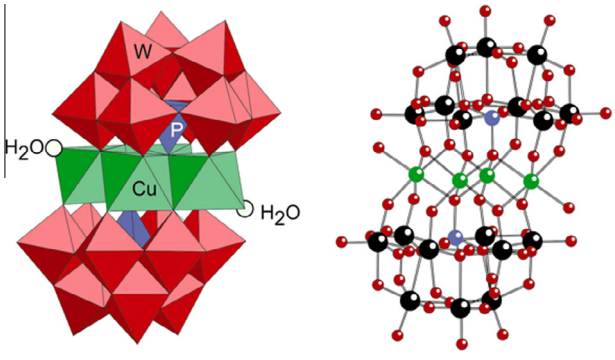

Fig. 1. Chemical structure of PW_9Cu.

3.3. Cytotoxicity studies

In order to get a deeper insight into the antiproliferative effects of the compound, its cytotoxicity on relevant organelles of the cells such as mitochondria and lysosomes, were investigated through the reduction of MTT and Neutral Red (NR) Uptake assays.

The MTT technique measures the ability of the mitochondrial succinic dehydrogenases to reduce the soluble yellow methyl tetrazolium salt to an insoluble blue MTT formazan product. Formazan is then solubilized and the absorbance measured spectrophotometrically [31].

The NR assay determines the uptake of the dye which accumulates in metabolically active lysosomes of uninjured cells [32].

3.3.1. MTT assay

The effects of PW_9Cu on the mitochondria metabolism of MG-63 osteosarcoma cells are shown in Fig. 3A. PW_9Cu caused an inhibitory effect from 25 to 100 μM with significant differences versus control ($p < 0.01$). The harmful action was the same between 25 and 100 μM showing no dose concentration effect in this range. These findings demonstrated the cytotoxic actions of PW_9Cu which affected the normal activity of the mitochondria, contributing to its deleterious effect on the tumor cell line MG-63.

3.3.2. NR uptake assay

The cytotoxic effect of PW_9Cu on the lysosome metabolism of MG-63 cell line was assessed by the NR uptake assay. For this purpose, concentrations ranging from 25 to 100 μM were used. Significant differences between treated cells and basal conditions were observed ($p < 0.01$) (Fig. 3B). These results showed a similar trend to those of the MTT and crystal violet assays suggesting that the cytotoxicity plays a crucial role in the antitumor actions of PW_9Cu.

3.4. Mechanisms of action

The putative cell death mechanisms triggered by the compound were investigated through the determination of the oxidative stress (ROS production), GSH levels and the redox couple GSH/GSSG. Moreover, an exhaustive study of apoptosis and cell cycle arrest were also performed.

3.4.1. Oxidative stress and GSH/GSSG status

The oxidative stress has been reported as one of the main factors that triggers deleterious actions of other metal compounds [41,42].

To understand the possible mechanism induced by PW_9Cu involved in the MG-63 cell death, we evaluated the effect of this compound on the oxidative stress through the ROS production and GSH/GSSG ratio.

ROS production was assessed by using DHR-123, a mitochondria-associated probe that selectively reacts with hydrogen peroxide [43]. Incubation of MG-63 osteosarcoma cells with PW_9Cu caused an increment on the ROS levels, as it can be observed in Fig. 4A. The compound increased ROS production in a dose-dependent manner with statistically differences from 25 to 100 μM

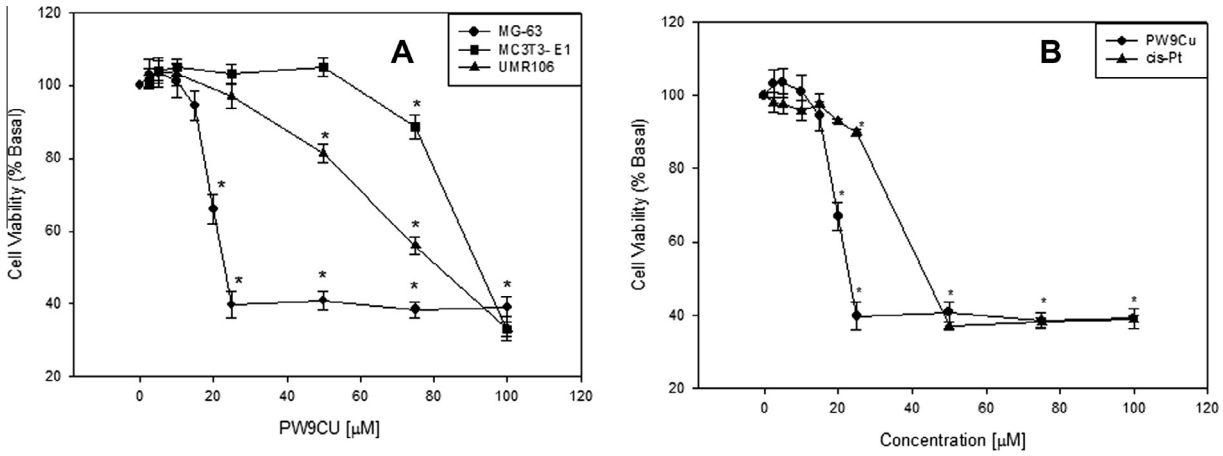

Fig. 2. (A) Effects of PW_9Cu on cell survival of three osteoblastic cell lines (MC3T3-E1, UMR106 and MG-63). (B) Effects of PW_9Cu and cis-Pt on cell survival in MG-63 cell line. Cells were incubated in serum-free DMEM alone (control) or with different concentrations of the compounds at 37 °C for 24 h. After incubation, cell survival was determined by the crystal violet assay. The results are expressed as the percentage of the basal level and represent the mean ± SEM ($n = 18$). *Significant difference in comparison with the basal level ($p < 0.01$).

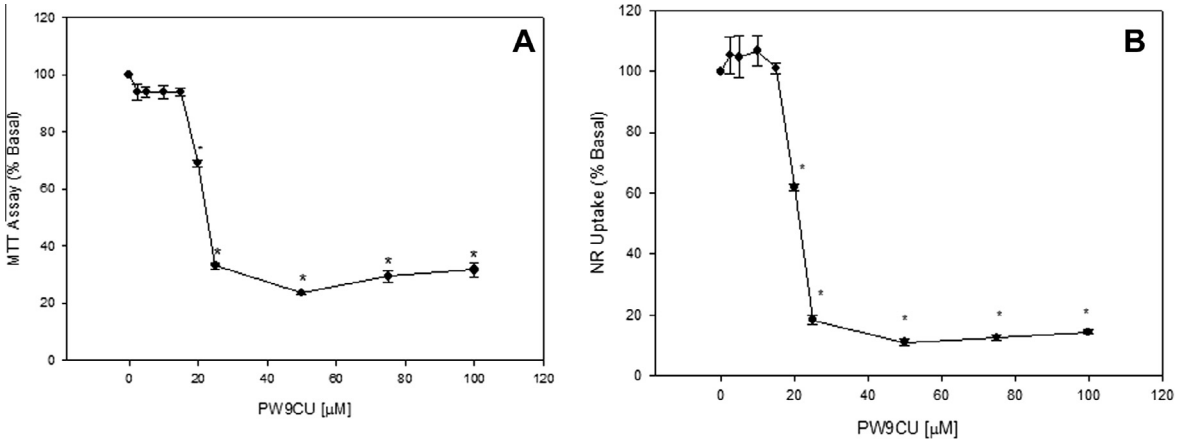

Fig. 3. (A) Evaluation of the mitochondrial succinate dehydrogenase activity by the MTT assay in MG-63 cells in culture. Cells were incubated with different doses of PW_9Cu for 24 h at 37 °C. After incubation, cell viability was determined by the MTT assay. Results are expressed as % basal and represent the mean ± SEM, $n = 18$, $^*p < 0.01$. (B) NR uptake by MG-63 osteosarcoma cells in culture. Cells were incubated with different concentrations of PW_9Cu for 24 h at 37 °C. After incubation, cell viability was determined by the uptake of NR. The dye taken up by the cells was extracted and the absorbance read at 540 nm. Results are expressed as % basal and represent the mean ± SEM, $n = 18$, $^*p < 0.01$.

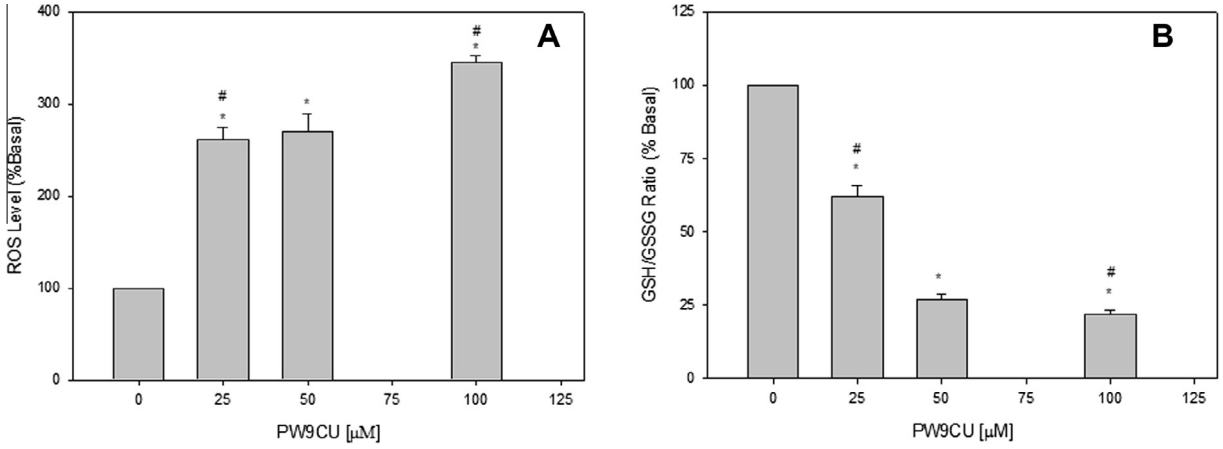

Fig. 4. (A) Induction of ROS by PW_9Cu in MG-63 cell line. Cells were incubated with growing concentrations of PW_9Cu at 37 °C for 24 h. ROS production in the cells was evaluated through the oxidation of DHR-123 to Rhodamine123. Results represent the mean ± SEM, $n = 12$, *significant differences vs. control ($p < 0.01$). #Significant differences between treatments ($p < 0.01$). (B) GSH/GSSG ratio in MG-63 cells, incubated with different concentrations of PW_9Cu. Results are expressed as mean ± SEM of three independent experiments, *significant differences vs. basal ($p < 0.01$), #significant differences between treatments ($p < 0.01$).

($p < 0.01$). At the highest concentration the complex caused 334% of ROS increment over basal, while at 25 μM, ROS production reached 255% over the control value. Statistical differences were determined between basal condition and these two concentrations ($p < 0.01$).

On the other hand, many authors have reported that reduced glutathione (GSH) plays a vital role in cellular function. GSH effectively scavenges free radicals and other reactive oxygen species directly and indirectly through enzymatic reactions [44]. In order to get a broader knowledge on the factors involved in the cellular redox status, the GSH/GSSG ratio was determined in the cultures of MG-63 cells incubated with different concentrations of PW_9Cu. A sustained increase in ROS levels may cause an accumulation of GSSG inside the cells. Because of this, the determination of GSH/GSSG ratio is relevant in the investigation of oxidative stress [45]. Fig. 4B shows the effect of PW_9Cu on the GSH/GSSG ratio. The compound induced a decrease in this ratio in the range of 25–100 μM ($p < 0.01$). In comparison to basal condition, at 25 μM of PW_9Cu, the value of GSH/GSSG ratio was 62% and while at 100 μM this ratio was 22% ($p < 0.01$). These results are in agreement with the data obtained in the ROS assay using these cells.

To confirm that the generation of ROS and the depletion of GSH played an important role in the cytotoxic effects, viability experiments were performed in the presence of the compound plus 1 mM GSH and with scavengers of ROS (vitamins C and E). The results can be seen in Fig. 5. At 25 μM of PW_9Cu, the surviving cells account for 40% in relation to the control, while in the presence of the thiol, this fraction was 95%, indicating a complete recovery in the presence of GSH. Besides, at 100 μM, the recovery caused by incubation of the cells with GSH, was only 19% of the basal. These results demonstrated the impact of the deleterious effect of the compound at the highest concentration (Fig. 5B). Similar results were observed in the Fig. 5A for a viability assay in the presence of an equimolar mixture of vitamin C and E.

As a whole, these results showed that the ROS generation and the decrease of GSH level may be, at least partly, some of the principal mechanisms of action involved in the deleterious effects of PW_9Cu.

3.4.2. Apoptosis study

Apoptosis is a physiological process of cell death enhanced in the presence of harmful agents. Programmed cell death is characterized by modifications of the plasma membrane, nuclear and/or cytoplasmic modifications and DNA fragmentation. Depending on the pathway that is triggered the molecular and structural changes involved might take place at different time points. In this work, three different methodologies have been used to characterize the apoptotic pathway induced by the compound.

3.4.2.1. Effects of PW_9Cu on PS externalization. Independently of the cellular type and the nature of the injuring agent, translocation of the phosphatidyl serine (PS) to the outer plasma membrane leaflet is one of the first events observed in apoptosis. Annexin V-FITC is a fluorescent probe with high affinity for PS allowing its determination by fluorescence assays.

Table 1 displays the quantification of apoptotic cells obtained by flow cytometry when MG-63 cells were treated with PW_9Cu (25 and 100 μM). After 24 h of incubation, control cultures presented 10% of Annexin V(+)/PI(−) cells and 7% of late apoptotic cells labeled as Annexin V(+)/PI(+). These percentages increased when the cells were treated with 100 μM of PW_9Cu, showing an increase in the late apoptotic fraction (63%) with a 27% of Annexin V(+)/PI(−) cells. On the contrary, the compound did not produce any effect on the cells at 25 μM. Thus, the percentages of apoptotic and apoptotic/necrotic cells increased in a dose dependent manner with PW_9Cu treatment.

3.4.2.2. Cell cycle analysis and DNA fragmentation. Cells go through the cell-cycle in several well-controlled phases [46]. The entry into each phase of the cell cycle is carefully regulated by different checkpoints. One issue emerging from drug discovery is to develop agents that target the checkpoints responsible for the control of cell-cycle progression.

Endonucleases activated during apoptosis target at internucleosomal DNA sections cause extensive DNA fragmentation [47]. On DNA content frequency histograms, the cells with deficit DNA content often form a characteristic 'sub-G1' or 'hypodiploid' peak [48].

When MG-63 cells were treated with PW_9Cu, several changes were observed in the cell cycle and apoptotic process in a dose dependent manner. With 25 μM of the compound, cell cycle arrest in G2/M phase was seen after 24 h of incubation (Fig. 6A). These phase still showed a significant increase after 48 h ($p < 0.01$). Moreover, it should be noted that under these experimental conditions no subG1 peak was detected. On the other hand, at 24 h with 100 μM concentration of PW_9Cu, the cells were conveyed to sub

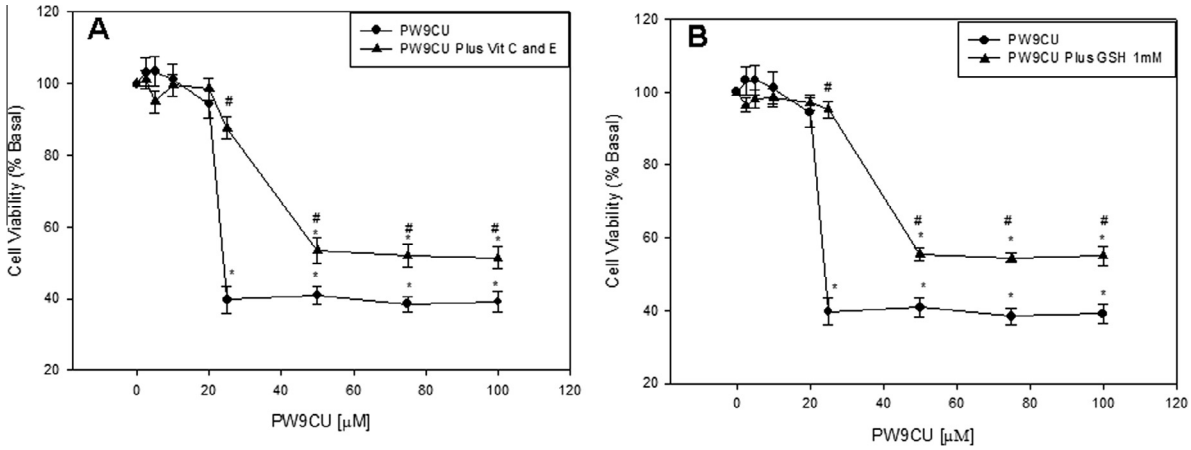

Fig. 5. (A) Effect of PW_9Cu on MG-63 cell viability in presence of GSH. Cells were incubated during 2 h with 1 mM GSH and then, different concentrations of the compound were added at 37 °C for 24 h. Results are expressed as the mean ± SEM, $n = 18$, *significant differences vs. control ($p < 0.01$). #significant differences between treatments ($p < 0.01$). (B) Effect of PW_9Cu on MG-63 cell viability in the presence of a mixture of vitamin C and E (50 μM each). Cells were incubated with different concentrations of the compound plus a mixture of vitamins C and E (50 μM each) during 24 h. Results are expressed as the mean ± SEM, $n = 18$, *significant differences vs. control ($p < 0.01$). #significant differences between treatments ($p < 0.01$).

Table 1
Percentage of apoptotic cells treated with PW_9Cu.

PW_9Cu (μM)	Annexin V (+) (%)	Annexin V (+) /PI (+) (%)
0	10	5
25	12	7
100	29*	66*

Results are expressed as mean ± SEM of three independent experiments, $n = 9$.
* Significant differences vs. control ($p < 0.01$).

G1 peak (Fig. 6B). Representative DNA content frequency histograms can be seen in Fig. 7.

The deleterious actions of PW9Cu were dose dependent and were intensified with the treatment time at elevated doses (see Figs. 6 and 7). The results suggest that the entry to the apoptotic process may take place through the cell cycle arrest, at one of the checkpoints that mediates the antiproliferative effect of PW_9Cu.

3.4.2.3. Morphological changes. Taking into account the harmful effects of PW_9Cu on cell viability, we next investigated the action of the compound on MG-63 cell morphology. After treatment during 6 or 24 h with both concentrations of PW_9Cu (25 and 100 μM), changes in cell morphology could be observed (Fig. 8). As expected, no alterations were observed in control cells. At 6 h, cells showed very well stained cytoplasms and oval nuclei. However, treatment with 25 μM produced slight alterations of the nuclear structure suggesting initial stages of fragmentation (Fig. 8B, see arrows). At 100 μM, a greater alteration in the cellular structure was observed in all the cells: the cytoplasms were scarce and condensed and the nuclei were condensed and fragmented. After 24 h of treatment, both concentrations (25 and 100 μM) caused high levels of fragmentation and condensation of the nuclei.

As a whole these results show a concentration dependent effect of morphological alterations in the cells treated with PW_9Cu, which is in agreement with the viability results. Moreover, the incubation time is also a factor that plays a significant role in the alterations of the cell morphology.

3.4.2.4. Mitochondrial membrane potential. Mitochondria are one of the more important organelles that can regulate cellular apoptosis [49,50]. The mitochondria transmembrane potential maintains the integrity and functions of the mitochondria. Dissipation of the MMP can lead the cells into apoptosis or necrosis [51].

To elucidate if PW_9Cu induced cytotoxicity in human osteoblasts by alterations of mitochondria functions, we evaluated the MMP in MG-63 cells under control conditions and in the presence of different concentrations (25, 50 and 100 μM) of PW_9Cu. The changes in MMP were measured by fluorescence spectroscopy using the probe Rhodamine 123. Fig. 9 shows the results for MG-63 cells. After 6 h of incubation only at 100 μM of PW_9Cu it could be observed a decreased of 25% in fluorescence intensity. Besides,

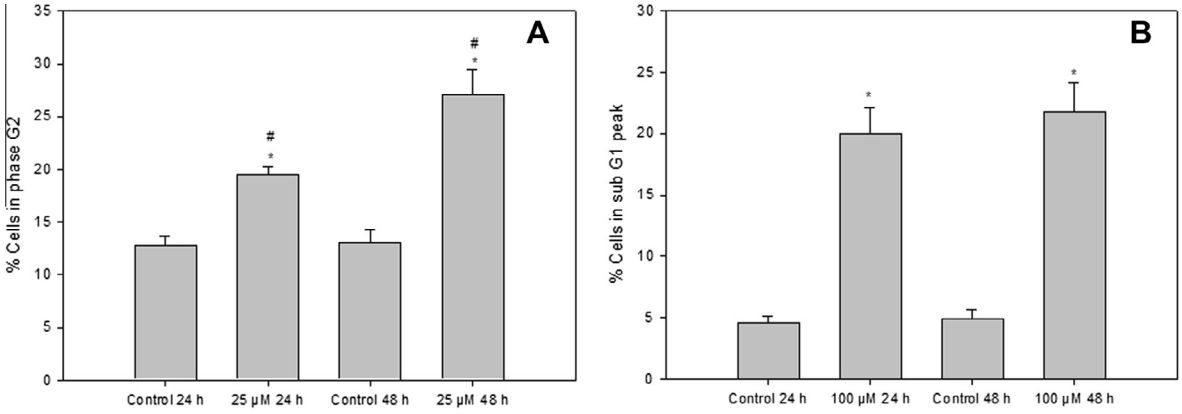

Fig. 6. Effect of PW_9Cu on cell cycle arrest and DNA fragmentation. (A) MG-63 cells were treated with 0 (control), and 25 μM of PW_9Cu at 37 °C during 24 and 48 h. Graphical bars show the percentage of G_2 phase cells. Results are expressed as the mean ± SEM, $n = 9$, *significant differences vs. control ($p < 0.01$), #significant differences between treatments ($p < 0.01$). (B) MG-63 cells were treated with 0 (basal) and 100 μM of PW_9Cu at 37 °C during 24 and 48 h. Graphical bars show the percentage of Sub G_1 peak cells. Results are expressed as the mean ± SEM, $n = 9$, *significant differences vs. control ($p < 0.01$), #significant differences between treatments ($p < 0.01$).

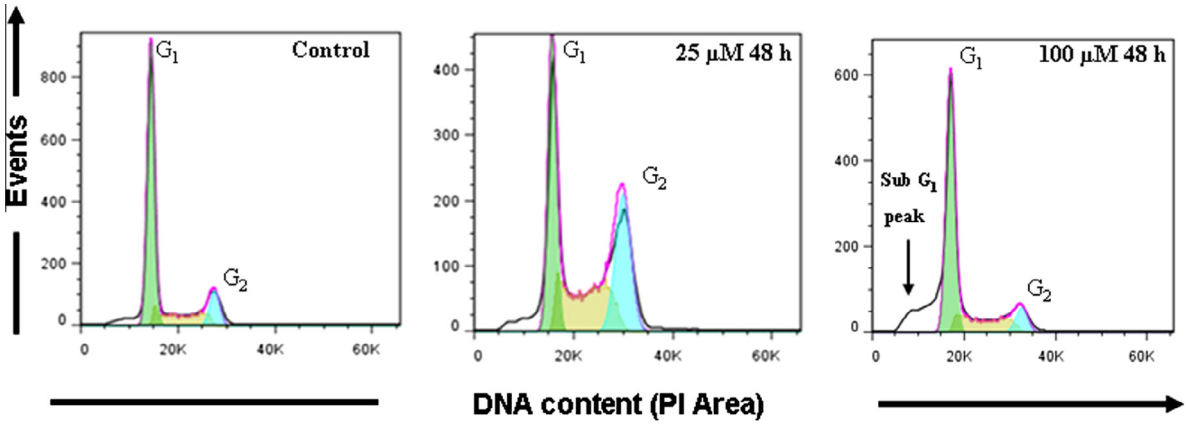

Fig. 7. Effect of PW_9Cu on cell cycle arrest and DNA fragmentation assessed by flow cytometry using PI stain. Examples of DNA content frequency histograms of cells treated during 48 h are shown and are representative of three independent experiments.

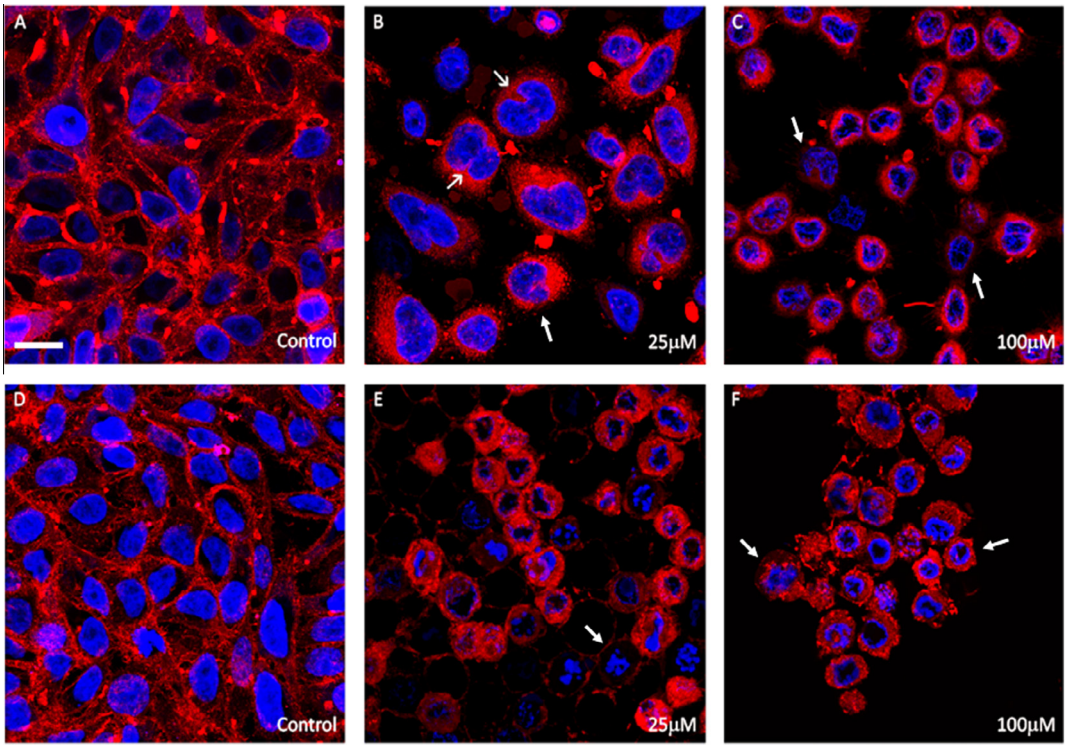

Fig. 8. PW_9Cu produces morphological changes in cells treated during 6 and 24 h. (A–C) MG-63 cells untreated or treated with 25 μM and 100 μM during 6 h. (A) Control cells showed a normal phenotipe of MG-G3 cells, (B) at 25 μM provoked slight alterations of the nuclear structure suggesting initial stages of apoptosis, (C) at 100 μM, a greater alteration in the cellular structure was observed in all the cells (see arrows). (D–F), MG-63 cells untreated or treated with 25 μM and 100 μM during 24 h. (D) Control cells showed very well stained cytoplasms and oval nuclei, (E and F) at 25 and 100 μM the compound caused high levels of DNA fragmentation and alterations of cell membrane (see arrows). TOPRO-3 is shown in blue and CellMask in red (scale bar = 20 μm). (For interpretation of the references to colour in this figure legend, the reader is referred to the web version of this article.)

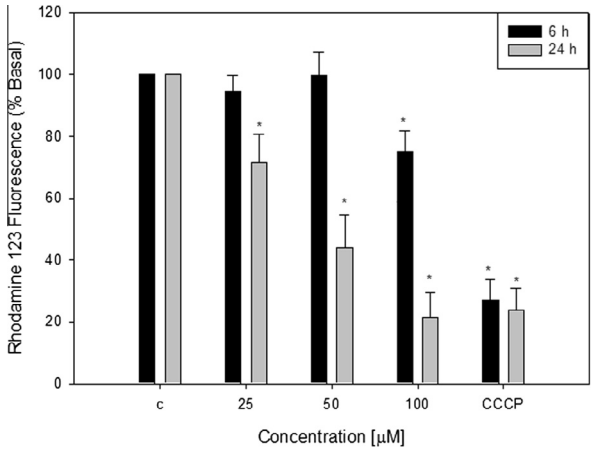

Fig. 9. Effect of PW_9Cu on Mitocondrial potential membrane (MMP). MMP was determined by the uptake of Rhodamine 123. MG-63 cells were treated with 0 (control), 25, 50 and 100 μM of PW_9Cu at 37 °C during 6 and 24 h. CCCP was used as a positive control of MMP dissipation. Graphical bars show the fluorescence units. The results are expressed as the percentage of the basal level and represent the mean ± SEM ($n = 9$). *Significant differences vs. control ($p < 0.01$).

the fluorescence intensity of Rhodamine 123 decreased, as the dose of the compound increased when the cells were incubated for 24 h indicating the dissipation of MMP. The values of fluorescence intensity were 71%, 44% and 23% for 25, 50 and 100 μM of PW_9Cu, respectively. The deleterious actions of PW_9Cu on MMP were dose dependent and also increased with the incubation time. The results suggest that the effects of the compound on MMP is, at least partly, one of the principal mechanism of action involved in the antitumoral actions of PW_9Cu.

4. Discussion

Cancer is one of the main death causes in the world, thus becoming a relevant issue of scientific investigation. Half of the men and one third of the women will develop some kind of cancer in their life. Osteosarcoma, one of the more common cancer of bone tissue, derives from bone-forming mesenchymal stem cells and may metastasize within the same extremity or to other organs, such as lung, liver, etc. [52]. To study the pharmacological activity of the metallodrug PW_9Cu we choose the MG-63 cell line (derived from a human osteosarcoma) because according to literature it is a good model for *in vitro* studies of bone cancer research [18,19].

Recently, there has been an increasing interest in the antitumor effects of HPOMs derivatives [53] since it has been previously demonstrated that these compounds exert a reduction of tumor growth *in vitro* systems [54–57].

As part of a research project devoted to the investigation of inorganic compounds with potential antitumor applications, we have tested the anticancer effects of PW_9Cu against osteosarcoma cells.

HPOMs based drugs are less expensive and easier to be obtained in large scale than most organic pharmaceuticals drugs. Their synthesis, characterization and biological properties as well as their mechanisms of action are of special scientific interest.

In this paper, we have investigated in detail the biological properties and the putative mechanisms of action of PW_9Cu.

Our results have demonstrated the selective antiproliferative effects of PW_9Cu in osteoblast cell lines. The compound caused the main deleterious action in tumoral cells than in the normal osteoblasts (MC3T3-E1 < UMR106 < MG-63, with IC_{50} values of: 92, 81 and 22 μM, respectively). On the other hand, the antitumor effects of PW_9Cu in human osteosarcoma cells were compared to

those of the reference antitumor drug *cis*-Pt. Nowadays, the anticancer platinum based drugs are among those most frequently used in the clinical practise. They have shown to be useful for the treatments of different tumors such as testicular, ovarian, bladder, lung, etc [58].

Our results showed the effectiveness of PW_9Cu as an alternative antitumor agent in the human osteosarcoma cell line MG-63 which a cell culture model for one of the more common form of bone cancer. In these cells PW_9Cu caused stronger deleterious action than *cis*-Pt as it can be seen from the comparison of the IC_{50} values (22 *vs*. 43 μM). These results indicate that PW_9Cu may be placed in the threshold of non platinum anticancer drugs and the compound is an interesting candidate for potential antitumor uses.

Moreover, our results showed that the cytotoxic effects of the compound on MG-63 cells may be due to different causes such as the disruption of several organelles like the lysosomes and the mitochondria. PW_9Cu affected their normal activity, contributing in this way to the deleterious effect of this compound on the tumor cell line MG-63. A similar trend was observed in MTT, NR and crystal violet assays suggesting that the cytotoxicity plays a crucial role in the antitumor actions of PW_9Cu.

In an attempt to elucidate the mechanisms of action involved in the effects of PW_9Cu, we studied the impact of the compound on oxidative stress generation and the redox status of the cells through the GSH/GSSG ratio. The compound increased ROS production in a dose-dependent manner. The relationship between ROS generation and cytotoxicity could be established by using a mixture of ROS scavengers (vitamin C + E). As it can be seen in Fig. 5A, the use of these scavengers significantly improved cell viability, demonstrating the relationship between oxidative stress and the deleterious action of the compound. Besides, it is generally known that GSH-related thiols participate in many important biological reactions, including the protection of cell membranes against oxidative damage. Our findings showed that PW_9Cu decreased GSH/GSSG ratio in the range of 25–100 μM with a dose effect between 25 and 50 μM while at 100 μM the value is similar to that of 50 μM. To establish the relevance of GSH in the maintenance of the redox status of the cells and its role in cell survival, we have added 1 mM of the thiol to the cultures with different concentrations of PW_9Cu. The beneficial effects of GSH were clearly demonstrated since the cell viability was totally recovered in the presence of 25 μM PW_9Cu and partially in the presence of higher concentrations of the drug. These results show that ROS generation and the decrease of GSH level may be, at least partially, some of the principal mechanisms of action involved in the antitumor effects of the PW_9Cu. Overall, it can be assumed that free radicals decrease the concentration of important cellular compounds and impair the antioxidant system making cells more vulnerable to oxidative damage. Similar results have been previously reported for other copper based drugs in cells in culture [59–62].

Finally, an exhaustive study of apoptosis and cell cycle analysis were also performed. There exist many reports in the literature about the incidence of high levels of ROS on the induction of apoptosis and cell cycle arrest [63,64]. In this work we have analysed these mechanisms using fluorescence spectroscopy, flow cytometry and confocal microscopy. PW_9Cu produced a cell cycle arrest at 25 μM while at 100 μM the cells were conveyed to death through apoptosis. Clearly, two mechanisms of action seem to be involved in the decrease of tumor cell survival. These mechanisms are dose dependent: at the lowest concentration the compound caused the arrest of the cell cycle at G_2/M phase while at the highest, PW_9Cu disrupted cell survival sending the tumor cells directly to programmed cell death. On the other hand, the compound provoked a disruption on the MMP after 24 h of incubation. Besides, the oxidative stress generated for the compound causes a dissipation of MMP which would be a "point of not return" that leads the cells to apoptosis. Taken into consideration all the techniques applied in our study it is worthy to mention that the cytotoxicity test showed different sensitivity in comparison with the method used to study the mechanism of action. In fact, the cytotoxicity is apparently the same at 25 and 100 μM since the sensibility of the cell viability methods (MTT, RN and crystal violet) are lower than those used in the mechanistic studies (fluorescence probes such us DHR123, rhodamine 123 TOPRO-3, CellMask). For this reason differences become evident when more sensible techniques are applied (FACS, confocal microscopy, fluorescence spectroscopy).

Studies carried out with the polyoxomolibdate PM-8 and PM-17 in pancreatic and gastric cancer cell lines also showed an increase in the number of apoptotic cells as a function of its concentration [55–57]. Besides, recent studies have shown that other HPOMs (decavanadates) tested on ovary and liver cancer cells, displayed cell cycle arrest in S phase as determined by flow cytometry [65].

Overall, our results demonstrate that ROS generation, GSH depletion, cell cycle arrest and apoptosis are the main processes that mediate the antiproliferative effect of PW_9Cu.

5. Conclusion

HPOMs are in the threshold to constitute a new group of non platinum anticancer drugs with potential application for alternative treatments in tumors. The major advantage of metal-based drugs is the ability to vary the coordination number, geometry, and redox states, which in turn, modify the pharmacological properties of these compounds.

A comprehensive study has been carried out for the first time on the promissory antitumor properties of the polyoxometalate PW_9Cu in a tumor osteoblastic cell line. We have clearly shown a more deleterious action of the compound in human osteosarcoma cells than in normal osteoblasts.

This investigation highlights the importance of oxidative stress, cell cycle arrest and apoptosis induced by HPOMs as the main mechanisms for antiproliferative actions and toxic effects. Finally, the interpretation of the *in vitro* biological data concerning PW_9Cu provides a better understanding of the bioprocess of this compound in tumor cells. This is a valuable rational basis for designing future experiments which will enable to establish its use in cancer treatments.

Conflict of Interest

The authors declare that there are no conflicts of interest.

Transparency Document

The Transparency document associated with this article can be found in the online version.

Acknowledgements

This work was partly supported by UNLP (11X/554), CONICET, (PIP 1125), ANPCyT (PICT 2008-2218 and PICT-2010- 0981) from Argentina. SBE is member of the Carrera del Investigador, CONICET, Argentina. CIC is member of the Carrera del Investigador, CIC, PBA. IEL has a fellowship from ANPCyT, Argentina and a fellowship from AMSUD- PASTEUR. MBF is member of the Sistema Nacional de Investigadores (SNI) of the Agencia Nacional de Investigación e Innovación (ANII) from Uruguay. The authors would like to thank Inés Tiscornia for the management work with the cells and Prof

Dr Gerardo Vasta for purchasing the Rhodamine 123 probe for the mitochondrial activity assay. Moreover, the authors would like to thank Prof. Maria del Carmen Bernal for her careful revision of the manuscript.

References

[1] M.T. Pope, Heteropoly and Isopoly Oxometalates, Springer, Verlag Berlin, 1983.
[2] J.T. Rhule, C.L. Hill, D.A. Judd, Chem. Rev. 98 (1998) 327–357.
[3] B. Hasenknopf, Front. Biosci. 10 (2005) 275–287.
[4] M. Raynaud, J.C. Chermann, F. Plata, C. Jasmin, G. Mathé, Science 272 (1971) 347–348.
[5] C. Jasmin, N. Raybaud, J.C. Chermann, D. Haapala, F. Sinoussi, C.B. Loustau, C. Bonissol, P. Kona, M. Raynaud, Biomedicine 18 (1973) 319–327.
[6] F. Bussereau, J.C. Chermann, E. De Clercq, C. Hannoun, Ann. Virol. 134 (1983) 127–134.
[7] M. Souyri-Caporale, G. Tovey, K. Ono, C. Jasmin, J. Chermann, J. Gen. Virol. 65 (1984) 831–835.
[8] O. Delgado, A. Dress, A. Muller, M.T. Pope, Polyoxometalates: A class of compounds with remarkable topology, in: M.T. Pope, A. Müller (Ed). Polyoxometalates: From Platonic Solids to Anti-Retroviral Activity, Kluwer Academic Publishers, Dordrecht, 1994.
[9] D. Rehder, Coord. Chem. Rev. 182 (1999) 297–322.
[10] P.J. Stankiewicz, A.S. Tracey, D.C. Crans, Vanadium and its role in life, in: H. Sigel, A. Sigel (Eds.), Metal Ions in Biological Systems, vol. 31, Marcel Dekker, New York, 1995.
[11] Y. Tajima, Curr. Top Biochem. Res. 4 (2001) 129–136.
[12] T. Yamase, N. Fukuda, Y. Tajima, Biol. Pharmacol. Bull. 19 (1996) 459–465.
[13] M. Jelikić-Stankov, S. Uskoković-Marković, I. Holclajtner-Antunović, M. Todorović, P. Djurdjević, J. Trace Elem. Med Biol. 21 (2007) 8–16.
[14] R. Raza, A. Matin, S. Sarwar, M. Barsukova-Stuckart, M. Ibrahim, U. Kortzc, J. Iqbal, Dalton Trans. 41 (2012) 14329.
[15] F. Pu, E. Wang, H. Jiang, J. Ren, Mol. BioSyst. 9 (2013) 113–120.
[16] M.T. Pope, A. Muller, Angew. Chem. Int. Ed. Engl. 30 (1991) 34–48.
[17] Z. Guo, P.J. Sadler, Adv. Inorg. Chem. 49 (2000) 183–306.
[18] A.B. Mohseny, I. Machado, Y. Cai, K.L. Schaefer, M. Serra, P.C. Hogendoorn, A. Llombart-Bosch, A.M. Cleton-Jansen, Lab. Invest. 91 (2011) 1195–1205.
[19] A.B. Mohseny, C.W. Pancras, C.W. Hogendoorn, A.M. Cleton-Jansen, Sarcoma (2012), http://dx.doi.org/10.1155/2012/417271.
[20] S.B. Etcheverry, P.A.M. Williams, Medicinal chemistry of copper and vanadium bioactive compounds, in: Ortega Marta P., Irene C. Gil (Eds.), New Developments in Medicinal chemistry, Nova science publishers, Inc., Hauppauge, NY, 2009, pp. 105–129 (Cap 5).
[21] J.R.J. Sorenson, in: R. Milanino, K.D. Rainsford, G.P. Velo (Eds.), Copper and Zinc in Inflammation, Kluwer Academic Publishers, Dordrecht, 1989, p. 69.
[22] G. Berthon, Agents Actions 39 (1993) 210–217.
[23] J.E. Weder, C.T. Dillon, T.V. Hambley, B.J. Kennedy, P.A. Lay, J.R. Biffin, H.L. Regtop, N.M. Davies, Coord. Chem. Rev. 232 (2002) 95–126.
[24] E. Frieden, Clin. Physiol. Biochem. 4 (1986) 11–19.
[25] J.R.J. Sorenson (Ed.), Biology of Copper Complexes, Humana Press, Clifton, NJ, 1987.
[26] R.G. Finke, M.W. Droegee, P.J. Domaillee, Inorg. Chem. 26 (1987) 3886–3896.
[27] S. Casuscelli, E. Herrero, M. Crivello, C. Pérez, M.G. Egusquiza, C.I. Cabello, I.L. Botto, Catal. Today 108 (2005) 230–234.
[28] M.G. Egusquiza, C.I. Cabello, I.L. Botto, H.J. Thomas, S. Casuscelli, E. Herrero, D. Gazzoli, Catal. Commun. 26 (2012) 117–121.
[29] T. Okajima, K. Nakamura, H. Zhang, N. Ling, T. Tanabe, T. Yasuda, R.G. Rozenfeld, Endocrinology 130 (1992) 2201–2212.
[30] A.M. Cortizo, S.B. Etcheverry, Mol. Cell. Biochem. 145 (1995) 97–102.
[31] T. Mosmann, J. Immunol. Methods 65 (1983) 55–63.
[32] E. Borenfreund, J.A. Puerner, J. Tissue Cult. Methods 9 (1984) 7–9.
[33] C.M. Krejsa, S.G. Nadler, J.M. Esselstyn, T.J. Kavanagh, J.A. Ledbetter, G.L. Schieven, J. Biol. Chem. 272 (1997) 11541–11549.
[34] M. Bradford, Anal. Biochem. 72 (1976) 248–254.
[35] P.J. Hissin, R. Hilf, Anal. Biochem. 74 (1976) 214–226.
[36] A.A. Hurley, Curr. Protoc. Cytom. (1997) 7.2.1–7.2.5.
[37] P. Pozarowski, J. Grabarek, Z. Darzynkiewicz, Curr. Protoc. Cytom. (2003) 7.19.1–7.19.33.
[38] E.Y. Wu, M.T. Smith, G. Bellomo, D. Di Monte, Arch. Biochem. Biophys. 282 (1990) 358–362.
[39] H. So, M.T. Pope, Inorg. Chem. 11 (1972) 1441.
[40] A.B.P. Lever, Inorganic Electronic Spectroscopy, second ed., Elsevier, Amsterdam, 1984.
[41] I.E. León, A.L. Di Virgilio, D.A. Barrio, G. Arrambide, D. Gambino, S.B. Etcheverry, Metallomics 4 (2012) 1287–1296.
[42] Z. Zhang, C. Huang, J. Li, S.S. Leonard, R. Lanciotti, L. Butterworth, X. Sh, Arch. Biochem. Biophys. 392 (2001) 311–332.
[43] M.A.M. Capella, L.S. Capella, R.C. Valente, M. Gefé, A.G. Lopes, Cell Biol. Toxicol. 23 (2007) 413–420.
[44] Y.Z. Fang, S. Yang, G. Wu, Nutrition 18 (2002) 872–879.
[45] C. Hwang, A.J. Sinskey, H.F. Lodish, Science 57 (1992) 1496–1502.
[46] C.J. Sherr, Cancer Res. 60 (2000) 3695–3698.
[47] S. Nagata, Exp. Cell Res. 256 (2000) 12–18.
[48] X. Huang, H.D. Halicka, F. Traganos, T. Tanaka, A. Kurose, Z. Darzynkiewicz, Cell Prolif. 38 (2005) 223–243.
[49] I. Herr, K.D. Debatin, Blood 98 (2001) 2603–2614.
[50] D. Grebenova, K. Kuzelova, K. Smetana, M. Pluskalova, H. Cajthamlova, I. Marinov, O. Fuchs, J. Soucek, P. Jarolim, Z. Hrkal, J. Photochem. Photobiol., B 69 (2003) 71–85.
[51] B. Mayer, R. Oberbauer, News Physiol. Sci. 18 (2003) 89–94.
[52] E. Kramarova, C.A. Stiller, Int. J. Cancer 68 (1996) 759–765.
[53] T. Yamase, Prog. Mol. Subcell. Biol. 54 (2013) 65–116.
[54] S. Dianat, A.K. Bordbar, S. Tangestaninejad, B. Yadollahi, S.H. Zarkesh-Esfahani, P. Habibi, J. Photochem. Photobiol., B 124 (2013) 27–33.
[55] S. Mitsui, A. Ogata, H. Yanagie, H. Kasano, T. Hisa, T. Yamase, M. Eriguchi, Biomed. Pharmacother. 60 (2006) 353–358.
[56] A. Ogata, S. Mitsui, H. Yanagie, H. Kasano, T. Hisa, T. Yamase, M. Eriguchi, Biomed. Pharmacother. 59 (2005) 240–244.
[57] A. Ogata, H. Yanagie, E. Ishikawa, Y. Morishita, S. Mitsui, A. Yamashita, K. Hasumi, S. Takamoto, T. Yamase, M. Eriguchi, Br. J. Cancer 98 (2008) 399–409.
[58] N.P. Farrell, Uses of Inorganic Chemistry in Medicine, Royal Soc Chem, UK, 1999.
[59] F. Bisceglie, S. Pinelli, R. Alinovi, P. Tarasconi, A. Buschini, F. Mussi, A. Mutti, G. Pelosi, J. Inorg. Biochem. 116 (2012) 195–203.
[60] M. Nagai, N.H. Vo, L. Shin Ogawa, D. Chimmanamada, T. Inoue, J. Chu, B.C. Beaudette-Zlatanova, R. Lu, R.K. Blackman, J. Barsoum, K. Koya, Y. Wada, Free Radic. Biol. Med. 52 (2012) 2142–2150.
[61] K.S. El-Gendy, M.A. Radwan, A.F. Gad, Chemosphere 77 (2009) 339–344.
[62] R. Alemón-Medina, J.L. Muñoz-Sánchez, L. Ruiz-Azuara, I. Gracia-Mora, Toxicol. In Vitro 22 (2008) 710–715.
[63] C.C. Wang, Y.M. Chiang, S.C. Sung, Y.L. Hsu, J.K. Chang, P.L. Kuo, Cancer Lett. 259 (2008) 82–98.
[64] H.K. Baumgartner, J.V. Gerasimenko, C. Thorne, L.H. Ashurst, S.L. Barrow, M.A. Chvanov, S. Gillies, D.N. Criddle, A.V. Tepikin, O.H. Petersen, R. Sutton, A.J.M. Watson, O.V. Gerasimenko, Am. J. Physiol. Gastrointest. Liver Physiol. 293 (2007) 296–307.
[65] F. Zhai, X. Wang, D. Li, H. Zhang, R. Li, L. Song, Biomed. Pharmacother. 63 (2009) 51–55.